Journal of Risk Analysis and Crisis Response, 2025, 15(2), 291-314
https://jracr.com/
ISSN Print: 2210-8491
ISSN Online: 2210-8505

Article

Integrated Framework for Detecting the Areas Prone to Flooding Using AHP in Bihar District, India

Simran Bharti [1], Gautam Kumar [1], Adyan Ul Haq [1,*] and L. T. S. Guite [1,*]

[1] Department of Geography, School of Environment and Earth Sciences, Central University of Punjab, Bathinda (151401), India
* Correspondence: adyangeo@gmail.com; Tel.: +918082349008 (A.U.H.); ltsguite@cup.edu.in; Tel.: +919612776850 (L.T.S.G.)

Received: February 27, 2025; Received in revised form: May 8, 2025; Accepted: June 16, 2025; Available online: June 30, 2025

Abstract: This study presents a comprehensive flood risk assessment framework that integrates physical hazard indicators with socio-economic vulnerability factors using the Analytical Hierarchy Process (AHP). Biophysical parameters such as elevation, slope, distance from rivers, rainfall, topographic wetness index (TWI), modified normalized difference water index (MNDWI), and normalized difference vegetation index (NDVI) were used to construct the Flood Hazard Zonation (FHZ), while demographic, land use/land cover (LULC), accessibility to essential services, and illiteracy rates informed the Flood Vulnerability Zonation (FVZ). AHP-derived weights ensured methodological rigor, with consistency ratio (CR) values of 0.0607 (FHZ) and 0.0329 (FVZ), both within acceptable limits (CR ≤ 0.1). The resultant Flood Risk Zonation (FRZ), derived from FHZ and FVZ integration, revealed significant spatial disparities: 8.30% of the area was classified as very low risk, 24.96% low, 31.00% moderate, 25.17% high, and 10.57% very high risk across a total area of 94,229.96 km². FHZ alone identified 31.05% of the region as very high hazard, while FVZ showed 33.04% of the area under moderate vulnerability. Urban zones exhibited elevated vulnerability due to population density and service dependency, whereas rural areas were more susceptible due to limited infrastructure and literacy. This multidimensional approach underscores the intricate interplay of environmental and human systems in shaping flood risks and offers a robust decision-support tool for spatial planning and disaster preparedness.

Keywords: Flood; Hazard; Vulnerability; AHP; Flood Risk; Disaster Risk Reduction; Bihar

1. Introduction

Flooding affects more people worldwide than any other danger and makes up around one-third of all disasters, making it one of the most common and destructive natural disasters [1,2]. Flooding is one of the most common and destructive natural disasters, especially in developing nations caused by inadequate drainage systems, low infiltration capacity, poor maintenance, unplanned urban growth, and human interventions all of which are made worse by climate and land-use changes are the main causes of its disastrous effects [3-5]. Flood frequency and intensity have increased in recent decades due to rapid urbanization, population development, and climate change, resulting in considerable economic losses, fatalities, and social disruptions [6,7]. Over the last 20 years, floods have killed 6,500 people and cost $15 billion in damage on average, highlighting the critical need for strong urban design and risk mitigation techniques [8]. Effective flood risk management requires

integrating hazard assessments with vulnerability assessments, recognizing that flood risk is caused by the interaction of flood hazards, which are defined by overflowing potential and intensity, as well as the vulnerability of people and infrastructure to unfavorable impacts [9,10]. In order to minimize damages, guide sustainable city development, and improve resilience to future flooding occurrences, hazard maps and risk assessments must be developed with a comprehensive understanding of flood severity, frequency, and the underlying conditioning factors.

India, which is frequently referred to as the "land of monsoons," is an ideal instance of how seasonal rains can be both advantageous and difficult [11]. Monsoons are important for the economy and agriculture, but they also carry a significant risk of flooding, which affects more than 32 million people each year [12]. Over 40 million hectares are designated as flood-prone, with areas such as the Brahmaputra and Ganga basins regularly experiencing devastating floods, evidenced by the 2018 Kerala floods and the statewide inundations in 2021 [13]. Bihar, a northeastern state accompanied by multiple rivers, is particularly susceptible, with its northern regions next to Nepal and the Terai region facing considerable flood hazards [14]. Between 2001 and 2018, districts such as Muzaffarpur, Katihar, and Saharsa had 16 flood years, while West Champaran had 15, highlighting the region's ongoing threat. According to loss and damage data from Bihar's disaster management agency, northern regions continue to be more susceptible to flooding than southern areas [15,16].

Numerous global as well as local threats of flooding studies have extensively used multi-criteria decision-making (MCDM), linked with GIS to designate flood hazard, susceptibility, and risk zones. MCDM approaches including AHP, FAHP, TOPSIS, Weights of Evidence (WoE), Frequency Ratio (FR), Logistic Regression (LR), and Multi-Layer Perceptron (MLP) are well-known models that have demonstrated efficacy in a variety of flooding scenarios [17-25].These methodologies provide precise assessment of flood-prone areas by systematically organizing alternatives based on defined criteria, allowing for decision making based on data and comprehensive flood management strategies [26,27].Notably, approaches like AHP, developed by Saaty (1980), and its integrations with GIS have demonstrated remarkable useful in flood risk studies [28-32]. AHP-based frameworks have been effectively used for hazard zonation, vulnerability assessments, and risk mitigation in flood-prone areas like northeast and central India by supporting paired comparisons and determining reciprocal values [33]. Such tools enhance the precision and applicability of flood hazard, vulnerability risk assessment [34]. To address such concerns, innovative approaches are required, such as mapping Flood Risk Zonation (FRZ) by combining Flood Hazard Zonation (FHZ) and Vulnerability Zonation (FVZ). Advanced methods such as multi-criteria decision-making (MCDM), combined with remote sensing and GIS technologies, provide precise recommendations that are consistent with worldwide frameworks for decreasing economic losses and increasing community resilience. This integrated methodology enables informed decision-making for designed mitigation strategies, thereby increasing long-term sustainability.

This study focuses on a comprehensive flood risk assessment system that incorporates hazard and vulnerability indicators to efficiently identify high-risk areas. The physical and ecological aspects of floods are measured by hazard indicators such elevation, slope, distance from rivers, rainfall, topographic wetness index (TWI), modified normalized difference water Index (MNDWI), and normalized difference vegetation index (NDVI).In addition to these, vulnerability indicators such as population, population density, land use/land cover (LULC), proximity to health institution, financial institution, roads, and railways, and illiteracy rates are used to assess the socioeconomic and

infrastructural conditions that influence communities' ability to cope with floods. These factors constitute an integrative framework for identifying high-risk locations and developing adapted flood mitigation techniques.

2. Materials and Methods

2.1. Study Area

Bihar, located in eastern India between 24° 20′ 10″ to 27° 31′ 15″ N latitude and 83° 19′ 50″ to 88° 17′ 40″ E longitude, is a landlocked state bordering Uttar Pradesh to the west, West Bengal to the east, Jharkhand to the south, and Nepal to the north (Figure 1). The state is divided into northern and southern plains by the Ganges River. The southern region is fed by rain-fed rivers like the Sone and Pun pun, while the northern region is dominated by Himalayan-origin rivers like the Gandak, Kosi and Bagmati, which carry heavy loads of sediment during monsoon seasons. Bihar's topography, combined with its large river systems, contribute to frequent and severe floods, which affects around 68,800 square kilometres of flood-prone areas each year. Flood risk reduction efforts, such building embankments and other structural measures, have frequently been criticized for their negative ecological and socioeconomic effects, which include aggravating riverbeds, altering natural flow patterns, and making places beyond embankments more vulnerable. Flood vulnerability is further increased by the state's socioeconomic profile, which is characterized by high population density, low per capita income, low levels of urbanization, and notable differences in literacy and development indices with a population of approximately 103.8 million, 90% of whom live in rural areas, Bihar's socioeconomic and environmental issues call for integrated, sustainable approaches to improve resilience and handle frequent flooding [35].

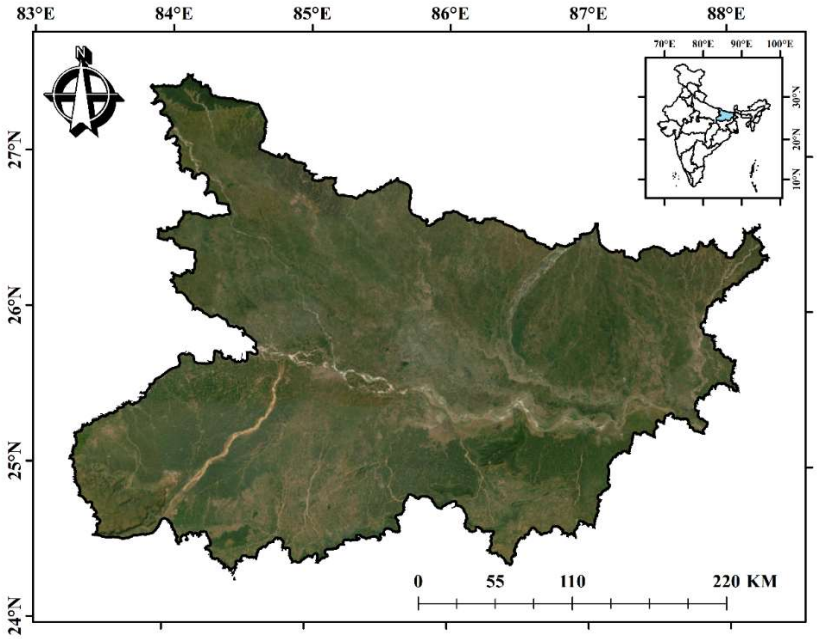

Figure 1. Location map of India and Study area, Bihar.

2.2. Data Collection and Preparation of Thematic Maps

The purpose of this study was to systematically evaluate and identify variables for flood hazard (FH) and flood vulnerability (FV) using comprehensive methodology. In order to achieve this, several

thematic data layers were extracted from valid datasets and processed using the ESRI ArcGIS 10.8. Elevation, slope, drainage network and the Topographic Wetness Index (TWI) were derived from the USGS SRTM dataset, a digital elevation model with a 30-meter spatial resolution, to create multiple thematic layers. NDVI and MNDWI indices were calculated using radiometrically corrected satellite imagery from the USGS LANDSAT-8, while Copernicus Open Access Hub provide Sentinel-2 imagery for Land Use/Land Cover (LULC) data. Rainfall data were obtained from the Climatic Research Unit (University of East Anglia) and Demographic as well as socioeconomic data, such as total population, illiteracy rate, and population density, were obtained from the 2011 Census of India and the Land Scan Global Population Database. Furthermore, spatial layers were created using OpenStreetMap data to indicate the proximity to health institution, roads, railways, and financial services. Table 1 summarizes and describes the variables used in the hazard and vulnerability zonation study.

Table 1. Indicators for Hazard and Vulnerability Zonation.

Indicators	Description	Year	Resolution	Source
Elevation, Slope, TWI and Proximity to Drainage	Derived from SRTM DEM	2023	30 m	United States of Geological Survey (USGS) https://earthexplorer.usgs.gov
NDVI and MNDWI	Landsat-8 OLI/TIRS	2023	30 m	
LULC	Sentinel-2	2023	10 m	Copernicus Open Access Hub https://scihub.copernicus.eu/
Rainfall	High resolution grided Data	2023	0.5° x 0.5°	Climate research unit https://crudata.uea.ac.uk/cru/data/hrg/
Population and Illiteracy rate	Obtaining the district-level data from Census of India, 2011	2011	-	Office of the Register General & Census Commissioner, India http://censusindia.gov.in/
Population Density	Lands can Population Data Global	2023	1 km	Oak Ridge National Laboratory (ORNL) https://landscan.ornl.gov/
Proximity to health institution, financial institution, roads and railways.	Obtained from OpenStreetMap	2023	-	OpenStreetMap Retrieved from: www.openstreetmap.org

Topographic wetness Index is derived from SRTM DEM using the Equation 1 [36]:

$$TWI=Ln(\frac{a}{\tan B}) \quad (1)$$

where a and B represents the specific catchment area and slope of the region, respectively.

MNDWI and NDVI both are calculated from the satellite image using the following Equation 2 and Equation 3 [37]:

$$\text{MNDWI} = \frac{\text{Green} - \text{Mir}}{\text{Green} + \text{Mir}} \quad (2)$$

$$\text{NDVI} = \frac{\text{NIR-RED}}{\text{NIR+RED}} \quad (3)$$

In Equation 2, the GREEN band reflects water bodies, while the MIR band helps distinguish water from land, as water absorbs MIR. While in Equation 3, the NIR band reflects healthy vegetation, while the RED band is absorbed by vegetation, helping to assess vegetation health.

2.3. Integrating Thematic Layers for Flood Risk Zonation (FRZ)

A GIS-based Multi-Criteria Decision Analysis (MCDA) approach has been utilized to delineate flood risk zones in Bihar. This methodology incorporates a variety of criteria, divided into two categories: flood hazard parameters and flood vulnerability indicators. To ensure a thorough assessment framework, seven factors have been identified for flood hazard analysis and eight indicators have been chosen to assess flood vulnerability. Together, these factors provide a comprehensive understanding of flood risks, allowing for more focused management and mitigation techniques.

Flood hazard mapping is based on a thorough analysis of key parameters that determine an area's being susceptible to floods. Elevation is a significant factor, with lower-lying locations being more prone to flooding due to increased river discharge and waterlogging [38-40]. Similarly, Slope has a major effect, as flatter terrains lower water flow velocity, increasing surface persistence and the rate of infiltration, therefore raising flood risk [41-43]. Another important indicator is the distance from rivers, as areas closer to river channels, particularly those in active floodplain zones, are more susceptible to flooding during peak flow events [44,45]. Topographic wetness index (TWI) helps identify locations prone to waterlogging by assessing soil moisture and water accumulation as impacted by slope and upstream contributions [46]. Furthermore, the modified normalized difference water index (MNDWI) improves flood susceptibility assessments by accurately identifying water bodies and low-lying terrains [47,48]. Rainfall intensity is a crucial indicator, with higher precipitation levels corresponding to increased surface runoff and flood risk [49,50]. Ultimately, the normalized difference vegetation index (NDVI) acts as an indirect indicator of flood susceptibility, as areas with sparse vegetation or negative NDVI values have lower water absorption and are more susceptible to floods [51]. Together, these variables (Figure 2) provide a framework for comprehensive flood hazard mapping, contributing in the identification of high-risk zones and the implementation of effective mitigation methods.

Flood vulnerability is strongly related to a variety of socioeconomic and infrastructural factors that enhance the effects of floods in vulnerable areas [52,53]. Population size is a vital factor since larger populations frequently pressure local resources and increase the chance of human exposure to flood threats [55-56]. Similarly, population density imposes more strain on land and infrastructure, making densely inhabited regions more vulnerable to disastrous flood damage due to overcrowding and restricted emergency alternatives [57-59]. Land Use and Land Cover (LULC) also play a crucial role because urbanization and land use changes shift the natural hydrological cycle, limiting infiltration capacity and increasing surface runoff [60,61]. Access to crucial services, such as medical

facilities and financial services, is equally important. Distances to hospitals and banks represent a community's readiness and resilience, with better proximity to these facilities allowing for more rapid response and recovery after floods [62]. Transportation infrastructure, is another important factor measured by distance to roads and railways, as inadequate or poorly maintained networks can hinder evacuation efforts and increase isolation in places that are vulnerable to flooding [63,64]. Illiteracy increases risk because education has a direct impact on awareness and adaptive capability; communities with greater literacy levels are more likely to implement preventive measures and respond successfully to flood threats [65,66]. Together, these indicators as shown in (Figure 3) provide a thorough understanding of flood vulnerability, emphasizing the importance of concentrated its efforts to reduce risks and strengthen resilience.

2.4. Decision Making: Weighting and Ranking via Analytical Hierarchy Process (AHP)

The Analytical Hierarchy Process (AHP), a Multi-Criteria Decision-Making (MCDM) method established by T. L. Saaty in the late 1970s, was originally utilized in the marketing sector [67-70]. Over time, it has grown to be one of the most popular techniques for assessing and ranking elements and categories over time, proving its usefulness in resolving challenging issues [71,72]. AHP is particularly valuable in flood hazard and vulnerability assessments due to its ability to address multi-faceted decision-making scenarios [66]. In this study, AHP was used to integrate various conditioning factors for flood susceptibility mapping, with each thematic layer's weight determined by its influence. Pairwise comparison matrices (PCM) were employed to compare the relative weight of factors within a theme and across different thematic layers. These weights were calculated using Saaty's scale (Saaty, 1980), which ranges from 1 to 9, based on expert opinions, field experience, and a comprehensive literature review. This knowledge-driven approach ensures that the weights assigned accurately represent the importance of each factor in determining flood hazard (FH) and vulnerability (FV). Despite the existence of alternative methods, AHP remains the preferred technique due to its consistency, efficiency, and cost-effectiveness. This study assigns weights to 15 factors (7 for FH and 8 for FV) using AHP, a novel method for calculating the Pairwise Comparison Matrix and evaluating its consistency ratio.

Table 2. Saaty scale of Importance.

Value	Importance Scale
1	Equal importance
2	Equal to moderate importance
3	Moderate importance
4	Moderate to strong importance
5	Strong importance
6	Strong to very strong importance
7	Very strong importance
8	Very to extremely strong importance
9	Extreme importance
1/1 to 1/9	Reciprocal values

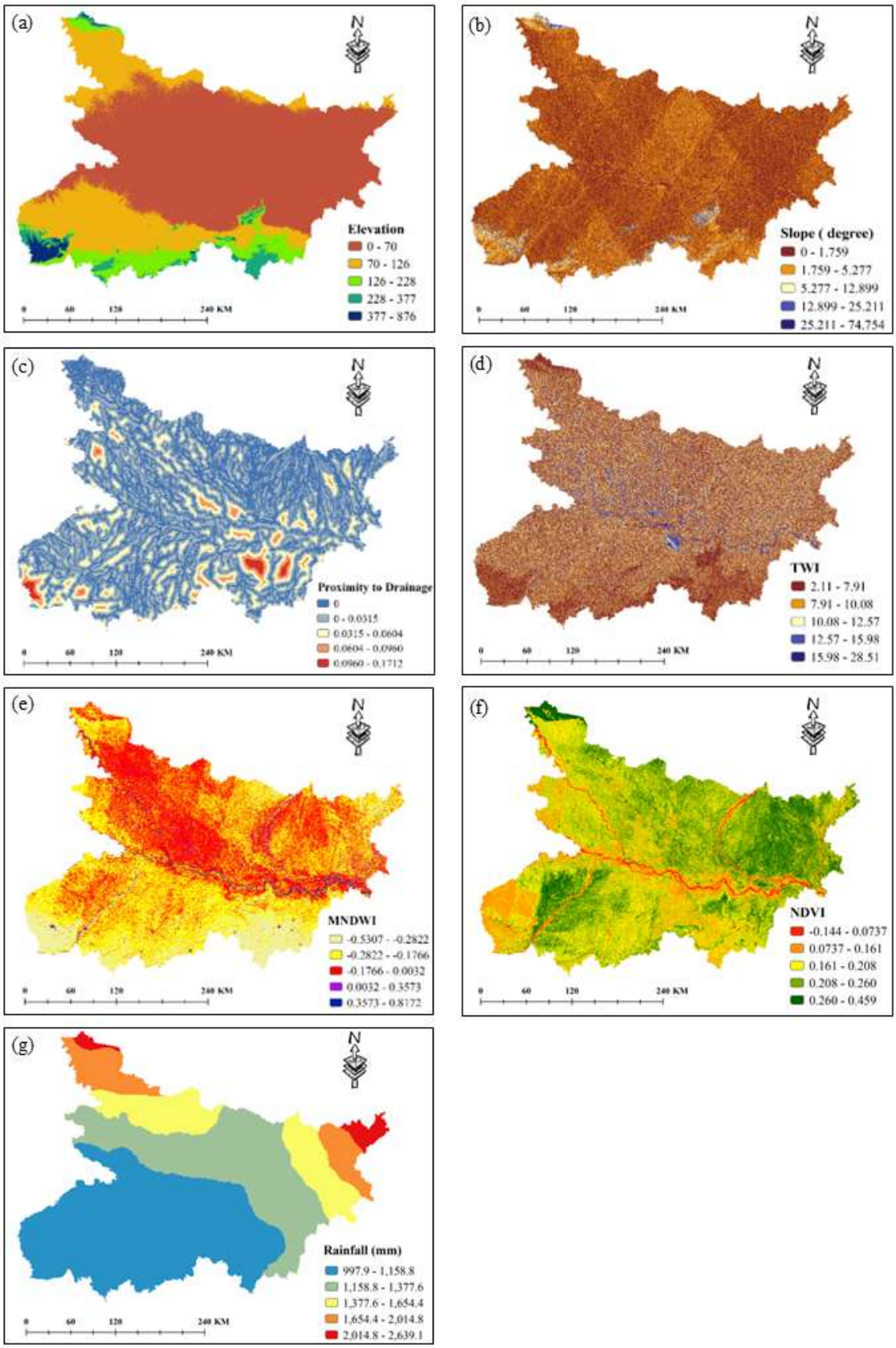

Figure 2. Flood hazard indicators of the Bihar: (a) elevation, (b) slope, (c) Proximity to drainage (d) Topographical wetness index (TWI), (e) modified normalized difference water index (MNDWI), (f) normalized difference vegetation index (NDVI), (g) Rainfall.

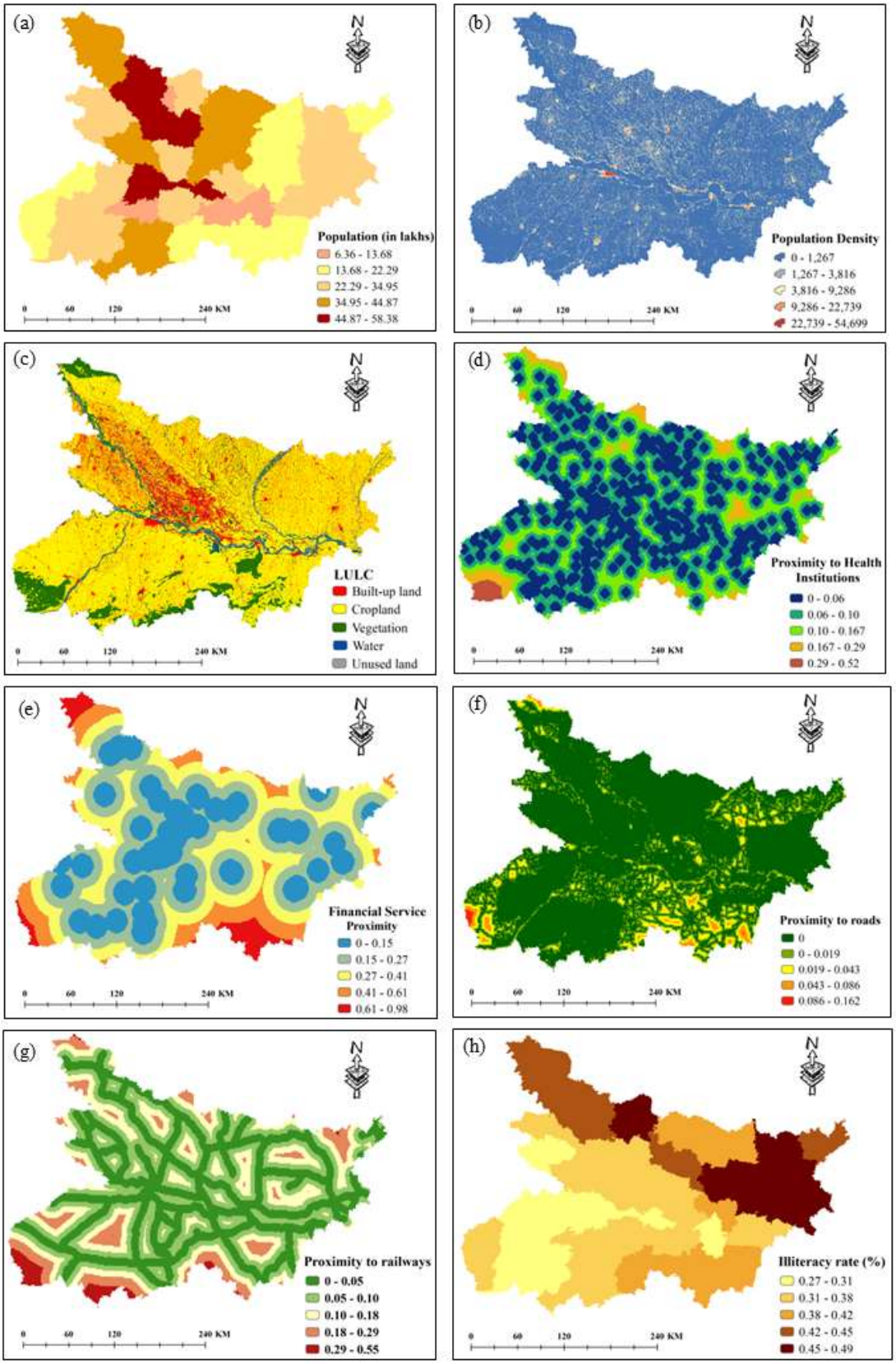

Figure 3. Flood Vulnerability indicators of the Bihar: (a) population (in lakhs), (b) population density, (c) land use land cover (LULC), (d) proximity to health institution, (e) financial service proximity (f) proximity to roads (g) proximity to railways, (h) Illiteracy rate (%).

The Analytic Hierarchy Process (AHP) technique creates a square matrix A = (a_{ij}) is constructed and comparing n criteria, representing both flood hazard characteristics (FHP) and flood vulnerability parameters (FVP). Each element of the matrix a_{ij} meets the requirement specified in Equation 4.

$$a_{ij} = 1/a_{ij} \tag{4}$$

In the case of reciprocal matrix, a_{ij} follow the equality, i.e.,

$$a_{ij} = \frac{P_i}{P_j}$$

where P_j denotes the preferences of the alternative i as stated in Equation 5.

$$A=\begin{pmatrix} \frac{P_1}{P_1} & \cdots & \frac{P_1}{P_j} & \cdots & \frac{P_1}{P_n} & \cdots \\ \frac{P_i}{P_1} & 1 & \cdots & 1 & \cdots & \frac{P_i}{P_n} \\ \ddot{P}_n & \cdots & \cdots & \frac{P_n}{P_j} & \cdots & \ddot{P}_n \\ \frac{}{P_1} & & & & & \frac{}{P_n} \end{pmatrix} \tag{5}$$

In this study seven Pairwise Comparison Matrix (PCM) for hazard zonation and eight for vulnerability zonation as shown in SM (Supplementary material). Subsequently, the relative ratio scale was calculated from the matrix derived through pairwise comparisons to determine the weights or ratings. The procedure involved the following steps:

Steps 1: Compute the sum up all the variable in the j column of matrix A using Equation 6.

$$\frac{P_1}{P_j}+\cdots+\frac{P_1}{P_J}+\cdots+\frac{P_n}{P_n}=\frac{\sum_{i=1}^{n} P_i}{P_j} \tag{6}$$

Step 2: Normalized Value are computed using Equation 7.

$$\frac{\frac{P_i}{P_j}}{\frac{\sum_{i=1}^{n} P_i}{P_j}}=\frac{P_1}{P_j}\times\frac{P_j}{\sum_{i=1}^{n} P_i}=\frac{P_i}{\sum_{i=1}^{n} P_i} \tag{7}$$

Step 3: Weight or rating (w_i) is calculated as the average of the elements using Equation 8.

$$W_i=\left(\frac{P_i}{\sum_{i=1}^{n} P_i}+\cdots+\frac{P_i}{\sum_{i=1}^{n} P_i}\right)\times\frac{1}{n} \tag{8}$$

2.5. Consistency Ratio

Assessing the consistency of judgments is fundamental to ensure the reliability and validity of the experts' decisions in the pairwise comparison process for each conditioning factor [18, 66]. The Consistency Ratio (CR) of the MCDM AHP model was determined by applying the Equation 9 and Equation 10 as outlined by Saaty (1988).

$$CR=\frac{CI}{RI} \tag{9}$$

Where CR represents the Consistency Ratio, CI denotes the Consistency Index, and RI is the Random Index, which is a constant value discussed in Saaty's work (1980b). The CI value was calculated using Equation 10 as follows:

$$CI=\frac{\lambda_{max}}{n-1} \tag{10}$$

Here, n represents the number of components and λ_{max} refers to the principal eigenvalue of the matrix, which was computed using Equation 11.

$$l_{max}=\sum_{i=1}^{n}\left(W_i\times\frac{P_i}{\sum_{i=1}^{n}P_i}\right) \tag{11}$$

Table 3. Random consistency index (RI).

n	1	2	3	4	5	6	7	8	9	10	11	12
R	0	0	0.58	0.9	1.12	1.24	1.32	1.41	1.45	1.49	1.51	1.48

If the CR value is ≤ 0.1, then the AHP results are considered acceptable. However, if the CR value exceeds 0.1, the results are deemed inconsistent, and the assessment method must be revised. The computed CR for flood susceptibility and vulnerability have been illustrated in Table 4, respectively.

Table 4. Consistency ratio for both Flood hazard zonation (FHZ) and Flood Vulnerability zonation.

	Lambda max	**N**	**CI**	**CR**
Flood Hazard Zonation	7.480727206	7	0.080121201	0.060698
Flood Vulnerability Zonation	8.325369327	8	0.046481332	0.032965

2.6. Mapping of Flood Hazard, Vulnerability and Flood Risk Zonation

The Flood Hazard (FH) and Flood Vulnerability (FV) parameters were weighted using the AHP methodology, taking into account the relative severity of each parameter. These weights were then applied in the cartographic representation on the ArcGIS platform, where the Spatial Analyst tool was used in conjunction with the weighted overlay technique. The Flood Hazard Zone (FHZ) and Flood Vulnerability Zone (FVZ) were calculated using Equation 12 and Equation 13, respectively.

$$FHZ=\sum_{i=1}^{n}w_i^h\times p_i^h \tag{12}$$

Here, FHZ represent FH zonation, W_i^h determine hazard indicators weights, P_i^h stand for the rank of hazard indicators.

$$FVZ=\sum_{i=1}^{n}w_i^v\times p_i^v \tag{13}$$

Here, FVZ represent FV zonation, W_i^v determine vulnerability parameters' weights, P_i^v stands for the rank of vulnerability indicators.

The main goal of this study is to create a flood risk zonation (FRZ) model. This objective was accomplished by combining the flood hazard zonation (FHZ) and flood vulnerability zonation (FVZ) maps through multiplication, as described in Equation 14.

$$FRZ = FHZ \times FVZ \quad (14)$$

3. Results

3.1. Flood Hazard Layers

The flood hazard analysis utilized elevation as a key parameter, classified into five categories: very low, low, moderate, high, and very high. The parameters of elevation, slope, proximity to drainage, topographic wetness index (TWI), modified normalized difference water index (MNDWI), Rainfall (mm) and Normalized Difference Vegetation Index (NDVI) play a critical role in determining flood hazard zonation as shown in Table 5 and Figure 4. Higher elevations (377-876 meters) are less vulnerable to flooding because they are elevated above flood-prone zones, whereas lower elevations (0-70 meters) are more vulnerable because they are closer to water sources and are more likely to be flooded. Flood risk is also influenced by slope; regions with very low slope (25.21° to 74.75°) are more likely to have more water accumulation and slower drainage, which raises the risk of flooding. On the other hand, regions with steeper slopes (0° to 1.76°) typically have faster drainage, which can lower the danger of flooding. Potential of flooding dangers is significantly influenced by the proximity to drainage networks. During periods of heavy rainfall, areas with a very high proximity to drainage is 39.88% are especially susceptible to flash floods and riverbank erosion. These areas frequently act as natural drainage channels, increasing runoff volume and velocity to the point where local hydrological systems are overloaded. On the other hand, because there aren't enough natural water outlets in places that are farther away from drainage systems where low proximity, covers only 0.80% of area, localized flooding may occur, particularly in impermeable or poorly managed environments.

The topographic wetness index (TWI) measures the potential for water accumulation, with high TWI areas range between 12.57 to 28.51, having an area of 12.94% indicating places at high risk of waterlogging and flooding. These areas are frequently low-lying and poorly drained, making them susceptible to extended flooding following heavy rains. Low TWI locations range from 2.11 to 7.91, as shown in Table 5 which cover area only 42.23% as shown in Table 5 are normally better drained, although flash floods can still occur if rainfall intensity exceeds infiltration capacity. The MNDWI helps detect water-rich areas and their sensitivity to hydrological risks. Wetlands, rivers, and other bodies of water that are naturally prone to flooding, particularly during peak discharge periods, are found in very high MNDWI zones especially 0.36 to 0.82 range, accounting for 1.34% of the total area. Meanwhile, moderate MNDWI zones lies between -0.18 to 0.0032, 37.49% of an area as shown in Table 5 are transitional locations where soil moisture levels can rise dramatically during heavy precipitation, raising the danger of surface runoff and localized floods. These places require careful management to strike a balance between environmental advantages and hazard mitigation.

Rainfall intensity and distribution play a critical impact in hazard susceptibility. Regions with extremely high rainfall 2014.8-2639.1 mm covering an area 2173.71 sq. km are especially vulnerable to flooding as shown in Table 5 and landslides, as heavy precipitation can saturate soils, impair cohesiveness, and enhance flow. Moderate rainfall zones 1158.8-1377.6 mm, having an area 13460.48 sq. km may face recurrent flooding, particularly in poorly drained or densely populated areas. Proper stormwater management is critical in these areas to reduce hazard hazards. Vegetation cover, as indicated by the normalized difference vegetation index, plays a crucial role in stabilizing soils and

reducing runoff. Areas with very high vegetation cover NDVI range 0.26–0.459, accounting for 14274.87 sq. km are less prone to erosion and flooding due to their ability to absorb rainfall and reduce surface runoff. In contrast, regions with low NDVI range -0.144–0.0737, covering 2.47% as shown in Table 5 are highly vulnerable to flooding and erosion due to sparse vegetation, which reduces the landscape's ability to buffer against extreme weather events (Table 5). Effective land management strategies, including afforestation and soil conservation, are necessary to mitigate these risks. These parameters collectively underscore the multifaceted nature of hazard susceptibility, emphasizing the need for integrated, location-specific approaches to risk assessment and management (Figure 4 (a)).

3.2. Flood Vulnerability Layers

Vulnerability assessment reveals how socio-economic, infrastructural, and demographic factors intersect to shape regional susceptibility to adverse outcomes during crises. Population distribution plays a pivotal role in vulnerability dynamics. Areas with very high population ranges 44.87–58.38 lakhs, covering 11.08% of the region are primarily urban zones, where dense populations increase dependency on infrastructure, heightening susceptibility to service disruptions and overburdened systems during emergencies. Conversely, areas with very low population counts ranges 6.36–13.68 lakhs, 5449.599 sq. km often lack access to critical resources, further isolating them and making emergency response challenging. Low population density areas (80.28%) may struggle with resource mobilization due to sparse infrastructure, while very high-density zones (0.16%) face unique challenges due to overcrowding and limited evacuation options. The distribution of land use and land cover (LULC) further elucidates vulnerability patterns. Urbanized built-up areas (16.31%) are highly vulnerable due to concentrated populations and critical infrastructure that can be easily overwhelmed during disasters. Croplands, which dominate the landscape (67.89%), indicate significant dependency on agriculture, rendering these regions particularly susceptible to environmental stresses that threaten livelihoods and food security. Water bodies (3.13%) introduce additional risks of flooding and waterborne diseases, especially in regions with underdeveloped infrastructure. Unused lands (1.18%) might seem low-risk but often lack basic amenities and accessibility, increasing vulnerability in emergencies.

Proximity to essential services such as healthcare and financial institutions underscore the disparities in access that drive vulnerability. A significant portion of the area (35.13%) has very low proximity to health services, primarily in rural regions where limited medical infrastructure delays emergency care. Financial service proximity follows a similar trend, with 29.87% of the area categorized as very low. This limited financial inclusion impacts recovery and resilience-building, leaving marginalized communities more vulnerable to prolonged adverse effects. Accessibility through transport networks also contributes to vulnerability. With 78.37% of the area having very low road proximity, these regions face significant barriers to evacuation and the timely delivery of relief services. Similarly, low railway connectivity (39.25%) highlights the isolation of many communities, further compounding their vulnerability during emergencies. Finally, the illiteracy rate amplifies vulnerability, particularly in areas with high illiteracy levels (0.42–0.49, accounting for 47.56% of the area). Education plays a critical role in disaster preparedness, risk awareness, and adaptive capacity. Communities in high-illiteracy zones are less likely to engage in effective risk reduction measures and often lack access to information crucial for resilience-building. Collectively, these

factors demonstrate the intricate interplay between socio-economic conditions and infrastructural inequities that shape the vulnerability landscape (Figure 4 (b)).

Table 5. Selected indicator for Flood Hazard Zonation (FHZ).

Parameter	Weight (%)	Reclass	Categories	Range	Area (Sq. km)	Area (%)
Elevation	0.33	5	very high	0 - 70	1197.198	1.270507
		4	high	70 - 126	2980.721	3.163242
		3	moderate	126 - 228	7194.501	7.635047
		2	low	228 - 377	24867.78	26.39053
		1	Very low	377 - 876	57989.75	61.54067
Slope	0.26	5	very high	0 - 1.759	348.7793	0.370136
		4	high	1.759 - 5.277	968.3105	1.027604
		3	moderate	5.277 - 12.899	2919.935	3.098734
		2	low	12.899 - 25.211	38240.39	40.58199
		1	Very low	25.211 - 74.754	51752.54	54.92154
Proximity to drainage	0.16	5	very high	0	37576.81	39.87777
		4	high	0 - 0.0315	46477.39	49.32337
		3	moderate	0.0315 - 0.0604	7316.757	7.764789
		2	low	0.0604 - 0.0960	2103.34	2.232135
		1	very low	0.0960 - 0.1712	755.6687	0.801941
Topographic wetness Index (TWI)	0.11	1	very low	2.11 - 7.91	39791.9	42.22851
		2	low	7.91 - 10.08	21133.85	22.42796
		3	moderate	10.08 - 12.57	21106.48	22.39891
		4	high	12.57 - 15.98	10125.92	10.74596
		5	very high	15.98 - 28.51	2071.799	2.198662
Modified Normalized Difference Water Index (MNDWI)	0.07	1	very low	-0.5307 - -0.2822	12524.84	13.29178
		2	low	-0.2822 - -0.1766	43017.53	45.65165
		3	moderate	-0.1766 - 0.0032	35327.99	37.49125
		4	high	0.0032 - 0.3573	2100.058	2.228652
		5	very high	0.3573 - 0.8172	1259.537	1.336663
Rainfall (mm)	0.04	1	very low	997.9 - 1,158.8	44657.68	47.39223
		2	low	1,158.8 - 1,377.6	25674.68	27.24684
		3	moderate	1,158.8 - 1,377.6	13460.48	14.28472
		4	high	1,654.4 - 2,014.8	8263.393	8.769391
		5	very high	2,014.8 - 2,639.1	2173.717	2.306821
Normalized Difference Vegetation Index (NDVI)	0.03	5	very high	0.260 - 0.459	14274.87	15.14898
		4	high	0.208 - 0.260	29762.41	31.58487
		3	moderate	0.161 - 0.208	30885.34	32.77656
		2	low	0.0737 - 0.161	16982.73	18.02264
		1	very low	-0.144 - 0.0737	2324.604	2.466948

Table 6. Selected indicator for Flood Vulnerability Zonation (FVZ).

Parameter	Weight	Reclass	Categories	Range	Area (Sq. km)	Area (%)
Population (in lakhs)	0.26	1	very low	6.36 - 13.68	5449.599	5.783298
		2	low	13.68 - 22.29	22943.67	24.34859
		3	moderate	22.29 - 34.95	33885.9	35.96086
		4	High	34.95 - 44.87	21509.07	22.82615
		5	very high	44.87 - 58.38	10441.71	11.0811
Population density	0.26	1	very low	0 - 1,267	75650.18	80.28252
		2	low	1,267 - 3,816	14191.92	15.06094
		3	moderate	3,816 - 9,286	3316.51	3.519592
		4	high	9,286 - 22,739	924.3691	0.980972
		5	very high	22,739 - 54,699	146.9797	0.15598
Land use Land cover (LULC)	0.17	1	very low	Water	2952.718	3.133523
		2	low	unused land	1112.871	1.181016
		3	moderate	vegetation	10827.01	11.48999
		4	high	cropland	63968.27	67.88528
		5	very high	built up	15369.09	16.31019
Proximity to Health Institution	0.12	1	very low	0 - 0.06	33106.9	35.13415
		2	low	0.06 - 0.10	34395.53	36.50169
		3	moderate	0.10 - 0.167	20568.64	21.82813
		4	high	0.167 - 0.29	5136.452	5.450976
		5	very high	0.29 - 0.52	1022.44	1.085047
Financial Services proximity	0.08	1	very low	0 - 0.15	28144.95	29.86837
		2	low	0.15 - 0.27	29716.8	31.53647
		3	moderate	0.27 - 0.41	22833.54	24.23172
		4	high	0.41 - 0.61	9719.427	10.31458
		5	very high	0.61 - 0.98	3815.243	4.048864
Proximity to road	0.05	1	very low	0	73847.31	78.36925
		2	low	0 - 0.019	14532.14	15.422
		3	moderate	0.019 - 0.043	4277.62	4.539554
		4	high	0.043 - 0.086	1261.29	1.338524
		5	very high	0.086 - 0.162	311.596	0.330676
Proximity to Railway	0.04	1	very low	0 - 0.05	36987.43	39.2523
		2	low	0.05 - 0.10	29163.68	30.94948
		3	moderate	0.10 - 0.18	17979.68	19.08064
		4	high	0.18 - 0.29	7978.315	8.466856
		5	very high	0.29 - 0.55	2120.852	2.250719
Illiteracy rate (%)	0.03	1	very low	0.27 - 0.31	21508.86	22.82593
		2	low	0.31 - 0.38	8305.497	8.814072
		3	moderate	0.38 - 0.42	19602.19	20.80251
		4	high	0.42 - 0.45	29598.15	31.41056
		5	very high	0.45 - 0.49	15215.25	16.14693

3.3. Flood Risk Zonation

Flood risk zonation (FRZ) is an integrated approach that combines hazard and vulnerability parameters, weighted according to their respective influence, to classify regions into five distinct flood risk categories: very low, low, moderate, high, and very high (Figure 4 (c)). Prior to the execution of the FRZ model, consistency ratios (CR) for each thematic layer and its sub-classes were calculated, demonstrating an acceptable level of consistency with CR values below 0.10, ensuring the reliability of the parameter classifications. After reclassifying the flood hazard and vulnerability layers and assigning appropriate weights, these layers were integrated into the ArcGIS10.8 platform using the weighted overlay method to generate the final flood risk zonation map for the study area. The final map was categorized into the five risk classes based on pixel values, with natural breaks classification techniques methods applied to distribute the flood risk zones. The high-risk zones, covering 9958.18 km², include districts such as Pashchim Champaran, Purbi Champaran, Samastipur, Patna, Madhubani, Sitamarhi, Muzaffarpur, Saran, and Darbhanga, which are prone to frequent and severe flooding, particularly during the monsoon, due to their proximity to the Gandak, Kosi, and Ganges rivers (Table 7). In contrast, the moderate-risk areas, spanning 29213.27 km², include districts like Supaul, Gopalganj, Gaya, Nalanda, Rohtas, Siwan, Begusarai, Khagaria, Vaishali, and Bhagalpur. These regions experience occasional flooding from river overflow and seasonal rainfall, impacting local agriculture, infrastructure, and communities, though they are less frequently inundated than the high-risk areas. Through the integration of hazard and vulnerability layers, this approach provided a thorough flood risk assessment, allowing for a detailed identification of flood-prone zones within the study area.

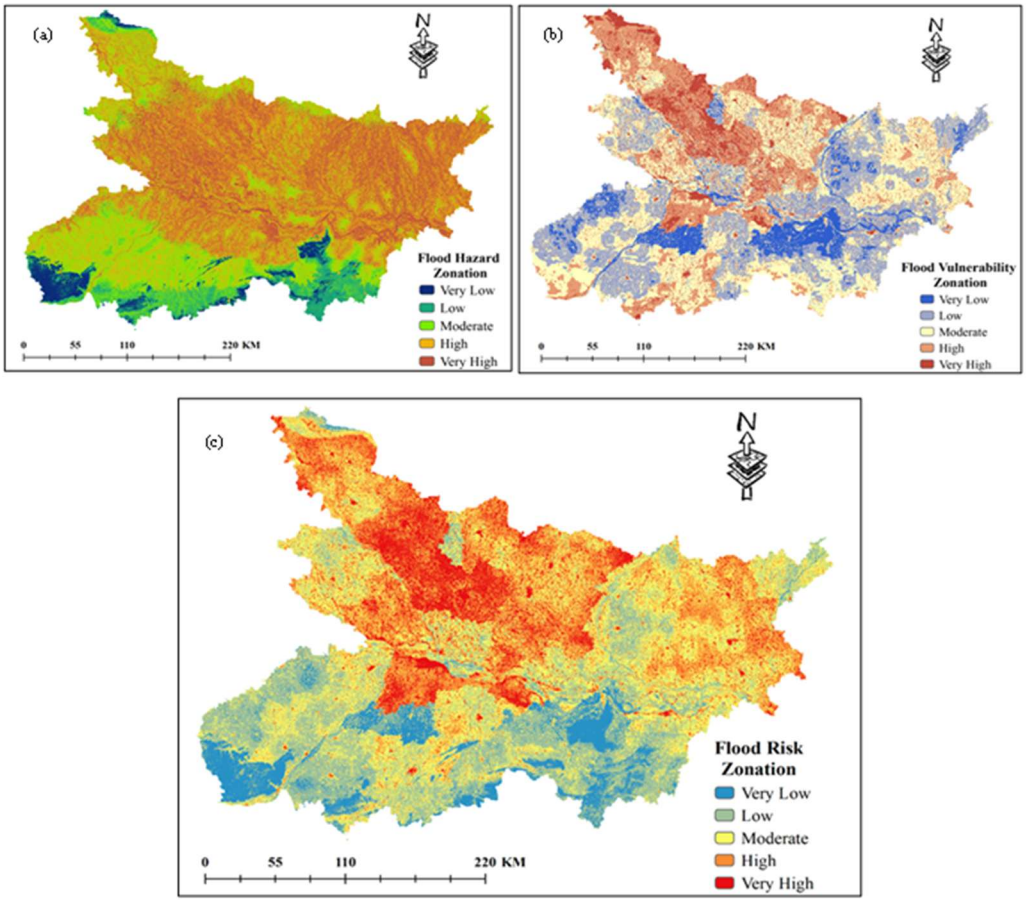

Figure 4. (a) Flood Hazard Zonation; (b) Flood Vulnerability Zonation; (c) Flood Risk Zonation mapping.

Table 7. Area of flood hazard, vulnerability, and risk zonation of Bihar State, India.

Category	FHZ			FVZ			FRZ		
	Range	*Area (Sq km)*	*Area (%)*	*Range*	*Area (Sq km)*	*Area (%)*	*Range*	*Area (Sq km)*	*Area (%)*
Very Low	1 - 2.6	3277.48	3.48	1.03 - 1.97	8522.04	9.04	1.92 - 6.89	7820.16	8.30
Low	2.6 - 3.29	6823.79	7.24	1.97 - 2.29	24320.94	25.81	6.89 - 8.65	23516.43	24.96
Moderate	3.29 - 3.76	19860.39	21.08	2.29- 2.58	31129.68	33.04	8.65 - 10.09	29213.27	31.00
High	3.76 - 4.14	35007.42	37.15	2.58- 2.92	21916.46	23.26	10.09 - 11.73	23721.92	25.17
Very High	4.14 - 5	29260.87	31.05	2.92 - 4.12	8340.82	8.85	11.73 - 18.59	9958.18	10.57
Total Area	-	94229.96	100	-	94229.96	100.00	-	94229.96	100.00

4. Discussion

This study employs the Analytical Hierarchy Process (AHP) to delineate flood hazard (FH), flood vulnerability (FV), and flood risk (FR) zones across Bihar State, India. By integrating multiple spatial and socio-environmental variables, AHP offers a structured and consistent decision-support framework that draws on expert opinion to assess and prioritize flood-related risks. Flood susceptibility in the region includes various factors such as topographic factors such as elevation and slope, hydrological elements like drainage density and river proximity, and terrain indices such as the Topographic Wetness Index (TWI). Flood vulnerability was further examined by incorporating demographic characteristics, land use and land cover (LULC), and accessibility to critical infrastructure, such as healthcare facilities. Previous studies by have established a clear relationship between flood vulnerability and proximity of settlements to riverbanks, indicating that populations residing closer to rivers are more susceptible to flood-related impacts [73-75].

In Bihar, the widespread lack of flood awareness and local understanding contributes to risky settlement patterns, where communities often establish homes and infrastructure within floodplains, thereby increasing their exposure to future flood hazards. The analysis of LULC patterns reveals that natural vegetation serves as a mitigating factor by reducing surface runoff velocity during floods. Conversely, areas with sparse vegetation particularly along riverbanks exhibit heightened flood susceptibility and erosion potential. As illustrated in Figure 2 (f), these vegetatively sparse zones are disproportionately at risk. Unregulated land use and rapid urban expansion, especially in the northwestern floodplain regions of Bihar, exacerbate vulnerability by increasing impermeable surfaces and decreasing natural water infiltration. This inverse relationship between land permeability and urbanization has been noted in other studies as well, reinforcing the argument that unplanned development significantly magnifies flood risk [76]. The findings align with prior research [77-82], which underscores vegetation loss as a major driver of increased flood vulnerability. Population density emerges as another critical determinant of vulnerability, particularly within high-exposure floodplains. Empirical evidence points to a positive correlation between population density

and flood risk, where densely populated areas often house more infrastructure, impervious surfaces, and socially marginalized populations [83-85]. Urban areas with higher densities typically face greater challenges in water infiltration due to widespread concrete and asphalt surfaces [83]. Moreover, vulnerable groups—such as low-income or marginalized communities—tend to be concentrated in these areas, further compounding exposure. Figure 4 (b) visually depict this pattern, showing heightened vulnerability in densely populated zones located within Bihar's floodplain. Nonetheless, strategic urban planning, flood-resilient infrastructure, early warning systems, and community engagement can play a pivotal role in reducing susceptibility, as supported by findings [76, 85]. At the core of this study lies the assessment of flood vulnerability, which, when integrated with hazard mapping, facilitates a comprehensive spatial flood risk analysis. Such an approach proves vital for identifying high, medium, and low-risk areas, thus enabling targeted interventions. Figure 4 (c) illustrates that more than half of Bihar's study region is highly vulnerable to flooding, largely due to unchecked LULC changes, deforestation, and the proliferation of substandard constructions within flood-prone zones.

This study demonstrates the successful integration of the AHP methodology in flood risk modelling by incorporating multiple criteria and expert judgment, this method offers a comprehensive and spatially explicit understanding of flood susceptibility, vulnerability, and risk. The application of Geographic Information Systems (GIS) and Multi-Criteria Decision-Making (MCDM) techniques proves to be a powerful tool in flood risk assessment, providing actionable insights for effective land-use planning and flood mitigation strategies. These findings are especially pertinent for regions sharing similar topographic and climatic conditions. Importantly, the study's results support the integration of vulnerability mapping into broader land use planning and disaster risk reduction strategies, aiding government and civil society efforts to achieve sustainable development and resilience against future flood events, especially in areas with limited data.

5. Conclusion and Its Future Scope

This research provides a comprehensive analysis of flood risk zones in Bihar by integrating flood hazard and vulnerability assessments through multiple indicators of exposure and susceptibility. The study identifies specific demographic groups such as women, children, the elderly, and individuals with disabilities as particularly vulnerable during flood events due to their limited mobility and increased presence in residential settings. Spatial patterns reveal that human-induced alterations to natural floodplains, especially for agricultural use, have significantly increased susceptibility in many regions. The encroachment into river basins has disrupted natural water flow, leading to heightened flood risks. As a result, the preservation of natural waterways, regulation of land use along flood-prone areas, and prohibition of high-risk agricultural activities are essential. Community-focused preparedness initiatives, especially training for pre-, during-, and post-flood responses, are vital to reduce disaster impact. Additionally, the flood vulnerability map developed in this study serves as a valuable decision-support tool for local authorities and planners, enabling more effective resource allocation and land-use management. A primary limitation of this study is the reliance on outdated data, specifically the 2011 Census of India, which is the most recent comprehensive demographic dataset available. The absence of updated census information restricts the ability to accurately capture recent developments such as population growth, urban expansion, infrastructural changes, and shifts in socio-economic conditions. These factors are critical for an accurate and current flood

risk assessment. The temporal gap between the data and the current ground reality presents challenges in modelling the dynamic and evolving nature of flood vulnerability. Furthermore, emerging climate trends and environmental changes key contributors to flood behaviour cannot be adequately addressed using static, decade-old data. The unavailability of more recent datasets limits the capacity to make high-resolution, real-time predictions or to develop adaptive strategies that reflect the latest ground conditions.

Advancements in data science and geospatial technologies present significant opportunities to enhance future flood risk assessments. The application of machine learning techniques such as Random Forest, Support Vector Machines, and Gradient Boosting can facilitate the classification and prediction of flood-prone areas based on diverse variables including elevation, land use, rainfall patterns, and socio-economic indicators. Deep learning models like Convolutional Neural Networks (CNNs) and Long Short-Term Memory (LSTM) networks offer powerful tools for analysing satellite imagery and time-series hydrological data to improve the accuracy of flood forecasting and early warning systems. Integrating these AI-driven approaches with real-time data from remote sensing, ground sensors, and IoT devices can support the development of dynamic flood monitoring platforms. These systems would allow stakeholders to visualize risk in real-time and take timely action. Future research should focus on incorporating such technologies alongside participatory planning, enabling both scientific precision and community empowerment in managing flood risks across Bihar.

Contributions: S.B.; conceptualization, project administration, data collection, formal analysis, data curation, supervision, resources, software, methodology, investigation, prepared all figures, writing –original draft, writing –review & editing. **G.K.**; data collection, formal analysis, visualization, writing –basic draft. **A.U.H.**; writing –review & editing, software, resources, methodology, project administration. **LT.S.G.**: project administration, data collection, formal analysis, supervision, resources, software, methodology, writing–original draft, writing –review & editing. All authors have read and agreed to the published version of the manuscript.

Funding: This research received no external funding.

Conflicts of Interest: The authors declare no conflict of interest.

Appendix A

Table A1. Decision matrix of the flood Hazard indictors for the AHP model.

Flood Hazard Indicator	Elevation	Slope	Proximity to drainage	TWI	MNDWI	Rainfall	NDVI
Elevation	1	2	3	4	5	6	7
Slope	1/2	1	3	4	4	6	7
Proximity to drainage	1/3	1/3	1	3	3	5	6
TWI	1/4	1/4	1/3	1	3	4	5
MNDWI	1/5	1/4	1/3	1/3	1	3	4
Rainfall	1/6	1/6	1/5	1/4	1/3	1	2
NDVI	1/7	1/7	1/6	1/5	1/2	0.5	1

Table A2. Decision matrix of the flood vulnerability indictors for the AHP model.

Flood Vulnerability Indicators	Population (in lakhs)	Population density	LULC	Proximity to health Institution	Proximity to financial services	Proximity to road	Proximity to railways	Illiteracy rate (%)
Population (in lakhs)	1	1	2	3	4	5	6	7
Population density	1	1	2	3	4	5	6	7
LULC	1/2	1/2	1	2	3	4	5	6
Proximity to health Institution	1/3	1/3	1/2	1	2	3	4	5
Proximity to financial services	1/4	1/4	1/3	1/2	1	2	3	4
Proximity to road	1/5	1/5	1/4	1/3	1/2	1	2	3
Proximity to railways	1/6	1/6	1/5	1/4	1/3	1/2	1	2
Illiteracy rate (%)	1/7	1/7	1/6	1/5	1/4	1/3	1/2	1

References

[1] Rentschler, J., Salhab, M., & Jafino, B. A. (2022). Flood exposure and poverty in 188 countries. Nature communications, 13(1), 3527. https://doi.org/10.1038/s41467-022-30727-4

[2] Jonkman, S. N., Curran, A. & Bouwer, L. M. (2024). Floods have become less deadly: an analysis of global flood fatalities 1975–2022. Nat Hazards, 120, 6327–6342. https://doi.org/10.1007/s11069-024-06444-0

[3] Singh, H., Nielsen, M., & Greatrex, H. (2023). Causes, impacts, and mitigation strategies of urban pluvial floods in India: A systematic review. International journal of disaster risk reduction, 93, 103751. https://doi.org/10.1016/j.ijdrr.2023.103751

[4] Agarwal, P., Sahoo, D., Parida, Y., Paltasingh, K. R., & Chowdhury, J. R. (2023). Land use changes and natural disaster fatalities: Empirical analysis for India. Ecological Indicators, 154, 110525. https://doi.org/10.1016/j.ecolind.2023.110525

[5] Asiedu, J. B. (2020). Reviewing the argument on floods in urban areas: A look at the causes. Theoretical and Empirical Researches in Urban Management, 15(1), 24-41. https://www.jstor.org/stable/26868293

[6] Agonafir, C., Lakhankar, T., Khanbilvardi, R., Krakauer, N., Radell, D., & Devineni, N. (2023). A review of recent advances in urban flood research. Water Security, 19, 100141. https://doi.org/10.1016/j.wasec.2023.100141

[7] Islam, M. Z., & Wang, C. (2024). Cost of high-level flooding as a consequence of climate change driver? A case study of China's flood-prone regions. Ecological Indicators, 160, 111944. https://doi.org/10.1016/j.ecolind.2024.111944

[8] Gupta, N., Dahal, S., Kumar, A., Kumar, C., Kumar, M., Maharjan, A., ... & Unni, A. (2021). Rich water, poor people: Potential for transboundary flood management between Nepal and India. Current Research in Environmental Sustainability, 3, 100031. https://doi.org/10.1016/j.crsust.2021.100031

[9] Zhu, Z., Zhang, S., Zhang, Y., Yao, R., & Jin, H. (2023). Integrating flood risk assessment and management based on HV-SS model: a case study of the Pearl River Delta, China. International journal of disaster risk reduction, 96, 103963. https://doi.org/10.1016/j.ijdrr.2023.103963

[10] Prall, M. C., Brandt, U. S., Halvorsen, N. S., Hansen, M. U., Dahlberg, N., & Andersen, K. J. (2024). A comprehensive approach for assessing social flood vulnerability and social flood risk: The case of Denmark. International Journal of Disaster Risk Reduction, 111, 104686. https://doi.org/10.1016/j.ijdrr.2024.104686

[11] Subrahmanyam, V. P. (1988). Hazards of floods and droughts in India. In Natural and Man-Made Hazards: Proceedings of the International Symposium held at Rimouski, Quebec, Canada, 3—9 August, 1986 (pp. 337-356). Springer Netherlands. https://doi.org/10.1007/978-94-009-1433-9_24

[12] Pal, S. C., Chowdhuri, I., Das, B., Chakrabortty, R., Roy, P., Saha, A., & Shit, M. (2022). Threats of climate change and land use patterns enhance the susceptibility of future floods in India. Journal of environmental management, 305, 114317. https://doi.org/10.1016/j.jenvman.2021.114317

[13] Vegad, U., Pokhrel, Y., & Mishra, V. (2023). Flood risk assessment for Indian sub-continental river basins. Hydrology and Earth System Sciences Discussions, 2023, 1-27. https://doi.org/10.5194/hess-28-1107-2024

[14] Senapati, S. (2022). Vulnerability and risk in the context of flood-related disasters: a district-level study of Bihar, India. International Journal of Disaster Risk Reduction, 82, 103368. https://doi.org/10.1016/j.ijdrr.2022.103368

[15] Bhatt, C. M., Gupta, A., Roy, A., Dalal, P., & Chauhan, P. (2021). Geospatial analysis of September, 2019 floods in the lower Gangetic plains of Bihar using multi-temporal satellites and river gauge data. Geomatics, Natural Hazards and Risk, 12(1), 84-102. https://doi.org/10.1080/19475705.2020.1861113

[16] Tripathi, G., Pandey, A. C., & Parida, B. R. (2022). Flood hazard and risk zonation in north Bihar using satellite-derived historical flood events and socio-economic data. Sustainability, 14(3), 1472. https://doi.org/10.3390/su14031472

[17] Debnath, J., Sahariah, D., Mazumdar, M. et al. (2023). Evaluating Flood Susceptibility in the Brahmaputra River Basin: An Insight into Asia's Eastern Himalayan Floodplains Using Machine Learning and Multi-Criteria Decision-Making. Earth Syst Environ, 7, 733–760. https://doi.org/10.1007/s41748-023-00358-w

[18] Ghosh, A., Chatterjee, U., Pal, S. C., Towfiqul Islam, A. R. M., Alam, E., & Islam, M. K. (2023). Flood hazard mapping using GIS-based statistical model in vulnerable riparian regions of sub-tropical environment. Geocarto International, 38(1), 2285355. https://doi.org/10.1080/10106049.2023.2285355

[19] Debnath, J., Sahariah, D., Nath, N. et al. (2024). Modelling on assessment of flood risk susceptibility at the Jia Bharali River basin in Eastern Himalayas by integrating multicollinearity tests and geospatial techniques. Model. Earth Syst. Environ., 10, 2393–2419. https://doi.org/10.1007/s40808-023-01912-1

[20] Sahraei, R., Kanani-Sadat, Y., Homayouni, S., Safari, A., Oubennaceur, K., & Chokmani, K. (2023). A novel hybrid GIS-based multi-criteria decision-making approach for flood susceptibility analysis in large ungauged watersheds. Journal of Flood Risk Management, 16(2), e12879. https://doi.org/10.1111/jfr3.12879

[21] Rincón, D., Khan, U. T., & Armenakis, C. (2018). Flood risk mapping using GIS and multi-criteria analysis: A greater Toronto area case study. Geosciences, 8(8), 275. https://doi.org/10.3390/geosciences8080275

[22] Danumah, J. H., Odai, S. N., Saley, B. M., Szarzynski, J., Thiel, M., Kwaku, A., ... & Akpa, L. Y. (2016). Flood risk assessment and mapping in Abidjan district using multi-criteria analysis (AHP) model and geoinformation techniques, (cote d'ivoire). Geoenvironmental Disasters, 3, 1-13. https://doi.org/10.1186/s40677-016-0044-y

[23] Rahmati, O., Pourghasemi, H. R., & Zeinivand, H. (2016). Flood susceptibility mapping using frequency ratio and weights-of-evidence models in the Golastan Province, Iran. Geocarto International, 31(1), 42-70. https://doi.org/10.1080/10106049.2015.1041559

[24] Shafapour Tehrany, M., Shabani, F., Neamah Jebur, M., Hong, H., Chen, W., & Xie, X. (2017). GIS-based spatial prediction of flood prone areas using standalone frequency ratio, logistic regression, weight of evidence and their ensemble techniques. Geomatics, Natural Hazards and Risk, 8(2), 1538-1561. https://doi.org/10.1080/10106049.2015.1041559

[25] Costache, R., Barbulescu, A., & Pham, Q. B. (2021). Integrated framework for detecting the areas prone to flooding generated by flash-floods in small river catchments. Water, 13(6), 758. https://doi.org/10.3390/w13060758

[26] Wang, L., Cui, S., Li, Y., Huang, H., Manandhar, B., Nitivattananon, V., ... & Huang, W. (2022). A review of the flood management: from flood control to flood resilience. Heliyon, 8(11). https://doi.org/10.1016/j.heliyon.2022.e11763

[27] Rathnasiri, P., Adeniyi, O., & Thurairajah, N. (2023). Data-driven approaches to build environment flood resilience: a scientometric and critical review. Advanced Engineering Informatics, 57, 102085. https://doi.org/10.1016/j.aei.2023.102085

[28] Ahmed, I., Pan, N. D., Debnath, J., Bhowmik, M., & Bhattacharjee, S. (2024). Flood hazard zonation using GIS-based multi-parametric Analytical Hierarchy Process. Geosystems and Geoenvironment, 3(2), 100250. https://doi.org/10.1016/j.geogeo.2023.100250

[29] Chen, Y. R., Yeh, C. H. & Yu, B. (2011). Integrated application of the analytic hierarchy process and the geographic information system for flood risk assessment and flood plain management in Taiwan. Nat Hazards, 59, 1261–1276. https://doi.org/10.1007/s11069-011-9831-7

[30] Dutta, P., & Deka, S. (2024). A novel approach to flood risk assessment: Synergizing with geospatial based MCDM-AHP model, multicollinearity, and sensitivity analysis in the Lower Brahmaputra Floodplain, Assam. Journal of Cleaner Production, 467, 142985. https://doi.org/10.1016/j.jclepro.2024.142985

[31] Hasanuzzaman, M., Adhikary, P. P., Bera, B., Shit, P. K. (2022). Flood Vulnerability Assessment Using AHP and Frequency Ratio Techniques. In: Pradhan, B., Shit, P. K., Bhunia, G. S., Adhikary, P. P., Pourghasemi, H. R. (eds) Spatial Modelling of Flood Risk and Flood Hazards. GIScience and Geo-environmental Modelling. Springer, Cham. https://doi.org/10.1007/978-3-030-94544-2_6

[32] Hagos, Y. G., Andualem, T. G., Yibeltal, M., et al. (2022). Flood hazard assessment and mapping using GIS integrated with multi-criteria decision analysis in upper Awash River basin, Ethiopia. Appl Water Sci, 12(7), 148. https://doi.org/10.1007/s13201-022-01674-8

[33] Gupta, L., & Dixit, J. (2022). A GIS-based flood risk mapping of Assam, India, using the MCDA-AHP approach at the regional and administrative level. Geocarto International, 37(26), 11867-11899. https://doi.org/10.21203/rs.3.rs-1015728/v1

[34] Mokhtari, E., Mezali, F., Abdelkebir, B., & Engel, B. (2023). Flood risk assessment using analytical hierarchy process: A case study from the Cheliff-Ghrib watershed, Algeria. Journal of Water and Climate Change, 14(3), 694-711. https://doi.org/10.2166/wcc.2023.316

[35] Bihar State Action Plan on Climate Change "Building Resilience through Development" Government of Bihar 2015. Accessed from https://moef.gov.in/uploads/2017/08/Bihar-State-Action-Plan-on-Climate-Change-2.pdf

[36] Sörensen, R., Zinko, U., & Seibert, J. (2006). On the calculation of the topographic wetness index: evaluation of different methods based on field observations. Hydrology and Earth System Sciences, 10(1), 101-112. https://doi.org/10.5194/hess-10-101-2006

[37] Ashok, A., Rani, H. P., & Jayakumar, K. V. (2021). Monitoring of dynamic wetland changes using NDVI and NDWI based landsat imagery. Remote Sensing Applications: Society and Environment, 23, 100547. https://doi.org/10.1016/j.rsase.2021.100547

[38] Almouctar, M. A. S., Wu, Y., An, S., Yin, X., Qin, C., Zhao, F., & Qiu, L. (2024). Flood risk assessment in arid and semi-arid regions using multi-criteria approaches and remote sensing in a data-scarce region. Journal of Hydrology: Regional Studies, 54, 101862. https://doi.org/10.1016/j.ejrh.2024.101862

[39] Al-Kindi, K.M., Alabri, Z. (2024). Investigating the Role of the Key Conditioning Factors in Flood Susceptibility Mapping Through Machine Learning Approaches. Earth Syst Environ, 8, 63–81. https://doi.org/10.1007/s41748-023-00369-7

[40] Shepherd, J. M. (2013). Impacts of urbanization on precipitation and storms: Physical insights and vulnerabilities. Climate Vulnerability, 5, 109-125. https://doi.org/10.1016/B978-0-12-384703-4.00503-7

[41] Osman, S. A., Das, J. (2023). GIS-based flood risk assessment using multi-criteria decision analysis of Shebelle River Basin in southern Somalia. SN Appl. Sci., 5, 134. https://doi.org/10.1007/s42452-023-05360-5

[42] Mu, W., Yu, F., Li, C., Xie, Y., Tian, J., Liu, J., & Zhao, N. (2015). Effects of rainfall intensity and slope gradient on runoff and soil moisture content on different growing stages of spring maize. Water, 7(6), 2990-3008.

[43] Morbidelli, R., Saltalippi, C., Flammini, A., & Govindaraju, R. S. (2018). Role of slope on infiltration: A review. Journal of Hydrology, 557, 878-886. https://doi.org/10.1016/j.jhydrol.2018.01.019

[44] Desalegn, H., & Mulu, A. (2021). Mapping flood inundation areas using GIS and HEC-RAS model at Fetam River, Upper Abbay Basin, Ethiopia. Scientific African, 12, e00834. https://doi.org/10.1016/j.sciaf.2021.e00834

[45] Tull, N., Moodie, A. J., & Passalacqua, P. (2024). River-floodplain connectivity and residence times controlled by topographic bluffs along a backwater transition. Frontiers in Water, 5, 1306481. https://doi.org/10.3389/frwa.2023.1306481

[46] Pourali, S.H., Arrowsmith, C., Chrisman, N. et al. (2016) Topography Wetness Index Application in Flood-Risk-Based Land Use Planning. Appl. Spatial Analysis, 9, 39–54. https://doi.org/10.1007/s12061-014-9130-2

[47] Laonamsai, J., Julphunthong, P., Saprathet, T., Kimmany, B., Ganchanasuragit, T., Chomcheawchan, P., & Tomun, N. (2023). Utilizing NDWI, MNDWI, SAVI, WRI, and AWEI for estimating erosion and deposition in Ping River in Thailand. Hydrology, 10(3), 70. https://doi.org/10.3390/hydrology10030070

[48] Ogilvie, A., Belaud, G., Massuel, S., Mulligan, M., Le Goulven, P., & Calvez, R. (2018). Surface water monitoring in small water bodies: potential and limits of multi-sensor Landsat time series. Hydrology and Earth System Sciences, 22(8), 4349-4380. https://doi.org/10.5194/hess-22-4349-2018

[49] Breinl, K., Lun, D., Müller-Thomy, H., & Blöschl, G. (2021). Understanding the relationship between rainfall and flood probabilities through combined intensity-duration-frequency analysis. Journal of Hydrology, 602, 126759. https://doi.org/10.1016/j.jhydrol.2021.126759

[50] Ramke, H. G. (2018). Collection of surface runoff and drainage of landfill top cover systems. Solid Waste Landfilling, 2018, 373-416. https://doi.org/10.1016/B978-0-12-407721-8.00019-X

[51] Hoang, D. V., & Liou, Y. A. (2024). Assessing the influence of human activities on flash flood susceptibility in mountainous regions of Vietnam. Ecological Indicators, 158, 111417. https://doi.org/10.1016/j.ecolind.2023.111417

[52] Roldán-Valcarce, A., Jato-Espino, D., Manchado, C., Bach, P. M., & Kuller, M. (2023). Vulnerability to urban flooding assessed based on spatial demographic, socio-economic and infrastructure inequalities. International journal of disaster risk reduction, 95, 103894. https://doi.org/10.1016/j.ijdrr.2023.103894

[53] Imran, M., Sumra, K., Mahmood, S. A., & Sajjad, S. F. (2019). Mapping flood vulnerability from socioeconomic classes and GI data: Linking socially resilient policies to geographically sustainable neighbourhoods using PLS-SEM. International Journal of Disaster Risk Reduction, 41, 101288. https://doi.org/10.1016/j.ijdrr.2019.101288

[54] Lowe, D., Ebi, K. L., & Forsberg, B. (2013). Factors increasing vulnerability to health effects before, during and after floods. International journal of environmental research and public health, 10(12), 7015-7067. https://doi.org/10.3390/ijerph10127015

[55] Ward, P. J., de Ruiter, M. C., Mård, J., Schröter, K., Van Loon, A., Veldkamp, T., ... & Wens, M. (2020). The need to integrate flood and drought disaster risk reduction strategies. Water Security, 11, 100070. https://doi.org/10.1016/j.wasec.2020.100070

[56] Bhattacharjee, K., & Behera, B. (2017). Forest cover change and flood hazards in India. Land use policy, 67, 436-448. https://doi.org/10.1016/j.landusepol.2017.06.013

[57] Leta, B. M., & Adugna, D. (2023). Characterizing the level of urban Flood vulnerability using the social-ecological-technological systems framework, the case of Adama city, Ethiopia. Heliyon, 9(10). https://doi.org/10.1016/j.heliyon.2023.e20723

[58] Borowska-Stefańska, M., Kowalski, M., Wiśniewski, S., & Dulebenets, M. A. (2023). The impact of self-evacuation from flood hazard areas on the equilibrium of the road transport. Safety science, 157, 105934. https://doi.org/10.1016/j.ssci.2022.105934

[59] Efraimidou, E., Spiliotis, M. (2024). A GIS-Based Flood Risk Assessment Using the Decision-Making Trial and Evaluation Laboratory Approach at a Regional Scale. Environ. Process, 11, 9. https://doi.org/10.1007/s40710-024-00683-w

[60] Kayitesi, N. M., Guzha, A. C., & Mariethoz, G. (2022). Impacts of land use land cover change and climate change on river hydro-morphology-a review of research studies in tropical regions. Journal of Hydrology, 615, 128702. https://doi.org/10.1016/j.jhydrol.2022.128702

[61] Kumar, M., Denis, D. M., Kundu, A., et al. (2022). Understanding land use/land cover and climate change impacts on hydrological components of Usri watershed, India. Appl Water Sci, 12, 39. https://doi.org/10.1007/s13201-021-01547-6

[62] Jamshed, A., Patel, C., Puriya, A., et al. (2024). Flood resilience assessment from the perspective of urban (in)formality in Surat, India: Implications for sustainable development. Nat Hazards, 120, 9297–9326. https://doi.org/10.1007/s11069-023-06267-5

[63] Markolf, S. A., Hoehne, C., Fraser, A., Chester, M. V., & Underwood, B. S. (2019). Transportation resilience to climate change and extreme weather events–Beyond risk and robustness. Transport policy, 74, 174-186. https://doi.org/10.1016/j.tranpol.2018.11.003

[64] Chen, X. Z., Lu, Q. C., Peng, Z. R., & Ash, J. E. (2015). Analysis of transportation network vulnerability under flooding disasters. Transportation research record, 2532(1), 37-44. https://doi.org/10.3141/2532-05

[65] Cerulli, D., Scott, M., Aunap, R., Kull, A., Pärn, J., Holbrook, J., & Mander, Ü. (2020). The role of education in increasing awareness and reducing impact of natural hazards. Sustainability, 12(18), 7623. https://doi.org/10.3390/su12187623

[66] Mitra, R., Saha, P., & Das, J. (2022). Assessment of the performance of GIS-based analytical hierarchical process (AHP) approach for flood modelling in Uttar Dinajpur district of West Bengal, India. Geomatics, Natural Hazards and Risk, 13(1), 2183-2226. https://doi.org/10.1080/19475705.2022.2112094

[67] Saaty, T. L. (1982). The analytic hierarchy process: A new approach to deal with fuzziness in architecture. Architectural Science Review, 25(3), 64-69.

[68] Saaty, T. L. (1995). Transport planning with multiple criteria: The analytic hierarchy process applications and progress review. Journal of advanced transportation, 29(1), 81-126. https://doi.org/10.1002/atr.5670290109

[69] Saaty, T. L. (2004). Decision making—the analytic hierarchy and network processes (AHP/ANP). Journal of systems science and systems engineering, 13, 1-35. https://doi.org/10.1007/s11518-006-0151-5

[70] Saaty, T. L. (2008). Decision making with the analytic hierarchy process. International journal of services sciences, 1(1), 83-98. https://doi.org/10.1504/IJSSCI.2008.017590

[71] Ullah, N., Tariq, A., Qasim, S. et al. (2024). Geospatial analysis and AHP for flood risk mapping in Quetta, Pakistan: a tool for disaster management and mitigation. Appl Water Sci, 14, 236. https://doi.org/10.1007/s13201-024-02293-1

[72] Kabenla, R., Ampofo, S., Owusu, G., et al. (2024) Application of Analytical Hierarchy Process (AHP) and Multi-Criteria Evaluation (MCE) for a case study and scenario assessment of flood risk in the White Volta Basin of the Upper East Region, Ghana. Discov Water, 4, 90. https://doi.org/10.1007/s43832-024-00143-4

[73] Chakrabortty, R., Pal, S. C., Malik, S., and Das, B. (2018). Modeling and mapping of groundwater potentiality zones using AHP and GIS technique: a case study of Raniganj Block, Paschim Bardhaman, West Bengal. Model. Earth Syst. Environ, 4, 1085–1110. https://doi.org/10.1007/s40808-018-0471-8

[74] Moreira, L. L., de Brito, M. M., and Kobiyama, M. (2021). Review article: a systematic review and future prospects of flood vulnerability indices. Nat. Hazards Earth Syst. Sci., 21 (5), 1513–1530. https://doi.org/10.5194/nhess-21-1513-2021

[75] Wang, B., Xu, G., Li, P., Li, Z., Zhang, Y., Cheng, Y., et al. (2020). Vegetation dynamics and their relationships with climatic factors in the Qinling Mountains of China. Ecol. Indic., 108, 105719. https://doi.org/10.1016/j.ecolind.2019.105719

[76] Ali, A., Ullah, W., Khan, U. A., Ullah, S., Ali, A., Jan, M. A., et al. (2023). Assessment of multi-components and sectoral vulnerability to urban floods in Peshawar–Pakistan. Nat. Hazards Res., 4(3), 507-519. https://doi.org/10.1016/j.nhres.2023.12.012

[77] Tanoue, M., Hirabayashi, Y., and Ikeuchi, H. (2016). Global-scale River flood vulnerability in the last 50 years. Sci. Rep., 6(1), 36021. https://doi.org/10.1038/srep36021

[78] Uddin, M. N., Islam, A. S., Bala, S. K., Islam, G. T., Adhikary, S., Saha, D., et al. (2019). Mapping of climate vulnerability of the coastal region of Bangladesh using principal component analysis. Appl. Geogr., 102, 47–57. https://doi.org/10.1016/j.apgeog.2018.12.011

[79] Sarkar, D., and Mondal, P. (2020). Flood vulnerability mapping using frequency ratio (FR) model: a case study on Kulik river basin, Indo-Bangladesh Barind region. Appl. Water Sci., 10 (1), 17–13. https://doi.org/10.1007/s13201-019-1102-x

[80] Ullah, K., and Zhang, J. (2020). GIS-based flood hazard mapping using relative frequency ratio method: a case study of Panjkora River Basin, eastern Hindu Kush, Pakistan. Plos one, 15(3), e0229153. https://doi.org/10.1371/journal.pone.0229153

[81] Luu, C., Von Meding, J., and Kanjanabootra, S. (2018). Assessing flood hazard using flood marks and analytic hierarchy process approach: a case study for the 2013 flood event in Quang Nam, Vietnam. Nat. Hazards, 90(3), 1031–1050. https://doi.org/10.1007/s11069-017-3083-0

[82] Li, Z., Song, K., & Peng, L. (2021). Flood risk assessment under land use and climate change in Wuhan city of the Yangtze River Basin, China. Land, 10(8), 878. https://doi.org/10.3390/land10080878

[83] Li, G. -F., Xiang, X. -Y., Tong, Y.- Y., and Wang, H. -M. (2013). Impact assessment of urbanization on flood risk in the Yangtze River Delta. Stoch. Environ. Res. Risk Assess, 27(7), 1683–1693. https://doi.org/10.1007/s00477-013-0706-1

[84] Shen, L., Wen, J., Zhang, Y., Ullah, S., Cheng, J., & Meng, X. (2022). Changes in population exposure to extreme precipitation in the Yangtze River Delta, China. Clim. Serv., 27, 100317. https://doi.org/10.1016/j.cliser.2022.100317

[85] Nasiri, H., and Shahmohammadi-Kalalagh, S. (2013). Flood vulnerability index as a knowledge base for flood risk assessment in urban area. J. Nov. Appl. Sci., 2 (8), 269–272. https://www.researchgate.net/publication/288612669_Flood_vulnerability_index_as_a_knowledge_base_for_flood_risk_assessment_in_urban_area

(Executive Editor: Li Wang)